



Eidgenössische Technische Hochschule Zürich
Swiss Federal Institute of Technology Zurich



SED

Schweizerischer Erdbebendienst
Swiss Seismological Service

Report on site characterization

Mettma, Germany (METMA)

Poggi Valerio, Lorenz Keller

Last modified - 24 / 12 / 2014

1. Introduction

In the framework of the NAGRA seismic network project, an active seismic survey was performed by the company RoXplore at the location of the SED station METMA (Mettma, Germany). The station, installed in a tunnel at about 46m below the surface, consists in a broadband seismometer (Trillium Compact) with a high-resolution digitizer (Taurus 24Bit @200sps). The scope of the survey is the seismic characterization of the rock mass surrounding the installation. The primary target is the definition of an equivalent one-dimensional shear-wave velocity. Such profile is later used to assess the local seismic response of the station.

For the analysis, different active seismic techniques have been employed, which are listed below:

- Seismic refraction (V_p and V_s) tomography
- Cross-hole tomography
- Active surface wave analysis (MASW)

Results from all these analyses were collected, merged and interpreted by SED into two separated summary profiles; one starting the free surface and one representative of the tunnel conditions. In the following, the main results of these investigations are summarized and a final interpretation of the velocity profile is given. From this interpretation, engineering parameters are finally derived, e.g. the Qwl- V_s average velocity, V_{sZ} (including V_{s30}) and the seismic amplification from the analytical SH-transfer function of the one-dimensional soil column.

2. Survey description

For the survey description and the processing results, we refer the reader to the RoXplore report in Appendix.

3. Soil type, topography and geology

From the geological points of view, the target area is characterized by an extended sandstone cover of Triassic age (unit 3 in **Figure 1**), on top of the Paleozoic granitic and high-grade metamorphic basement of the black forest (unit 1). Triassic shellbearing limestone (unit 2) is also occasionally present in the surroundings, however not visible at the measuring location. Topography is smooth and modeled by the action of glaciers during Pleistocene. Such site can be classified as of rock ground-type A.

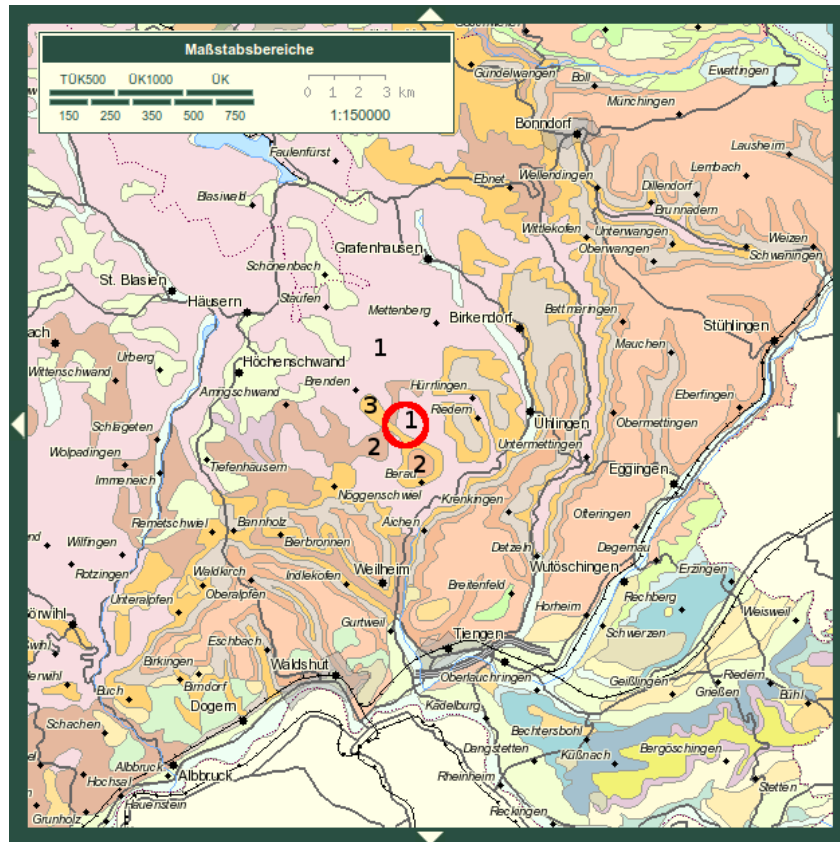


Figure 1 - Geological map of the southern edge of the Black Forest (reproduced from Landesamt für Geologie, Rohstoffe und Bergbau (LGRB) Freiburg, modified). In red the approximate location of the permanent station EMMET.

4. Profile selection

From the ensemble of all S-wave velocity profiles provided by RoXplore from the different applied seismic techniques (refraction tomography, cross-hole tomography and MASW analysis) a number of best models have been selected (**Figure 2**). These profiles are considered the most representative of the local geophysical conditions, spanning from the free-surface to about 35m below the station installation (in the tunnel). The selected profiles have however different resolution characteristics and depth extension (depending on the technique used for the analysis) and therefore they cannot easily be compared or simply averaged into a unique mean profile. We proceeded by generating a final V_s “summary” model by visual inspection and then manual interpretation of the available data at the different depths.

Calibration of a P-wave velocity model is a more complex task, because of the limited amount of usable information. Practically, V_p profiling is available only from refraction P-wave seismic surveying and active MASW analysis. In the former case, however, the maximum resolved depth is not sufficient to reach the depth of the station (in the tunnel). In case of MASW, conversely, the V_p values obtained by surface wave inversion are always quite uncertain, due to the scarce sensitivity of this parameters, and should therefore be used carefully. We then proceeded by calibrating an average V_p - V_s relation using log-linear regression on a sub-selection of the available data (**Figure 3**). The functional relation was then used to directly convert the previously obtained V_s model into a unique V_p profile (**Figure 4**). This procedure was applied to obtain two complementary models, one ranging from the surface to below the tunnel (**Figure 4A**) and a second profile more specific for the conditions below the station (**Figure 4B**).

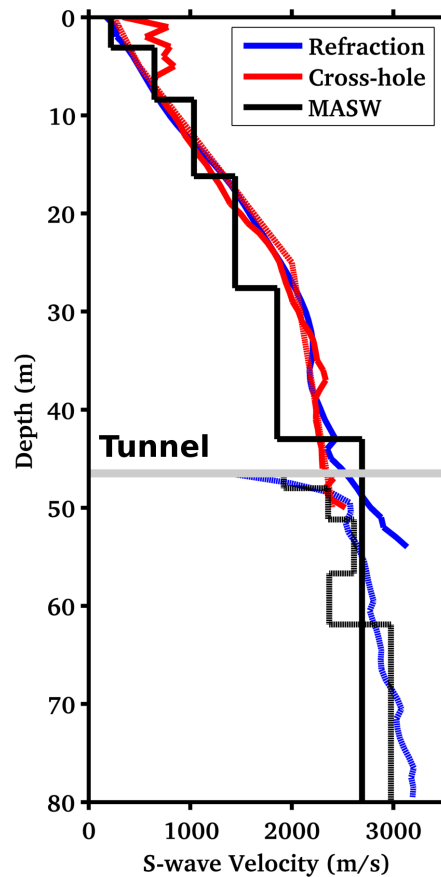


Figure 2 - Ensemble of selected “best” V_s profiles from different techniques at the location of the seismic station METMA. Note that the refraction profile (in blue) is discontinuous because obtained from two independent surveys (at the surface and in the tunnel).

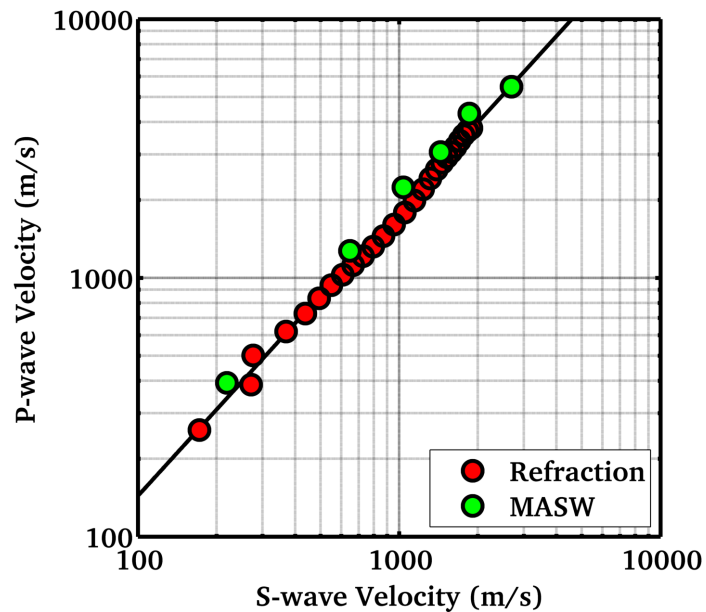
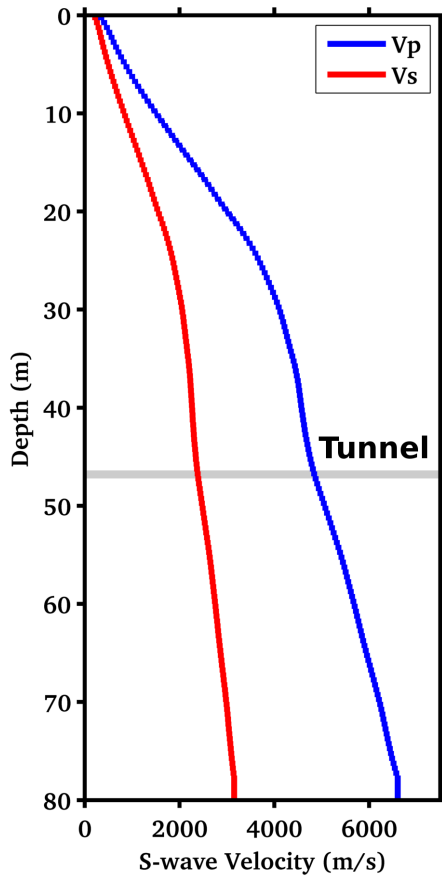


Figure 3 - Calibration of log-linear regression relation between *P* and *S* seismic velocities. Calibration data are from a selection of refraction profiles and from the best MASW model (Rayleigh and Love wave joint inversion).

5. Engineering soil parameters

The obtained best velocity profile is then used to derive average soil parameters like the V_sZ (average travel-time S-wave velocity over the depth Z , including V_{s30} , Table 1) and the quarter-wavelength (QWL) average velocities (Joyner et al., 1984) for a range of frequencies between 0.6 and 30Hz (**Figure 5** and **Figure 6**). The former is a standard parameter for the classification of ground-types in most building codes and in ground motion prediction equations. The latter is a parameter useful for the empirical estimation of the site-response and to assess the sensitivity of the seismic wave-field to the different depths.

A) Free-surface profile



B) Tunnel profile

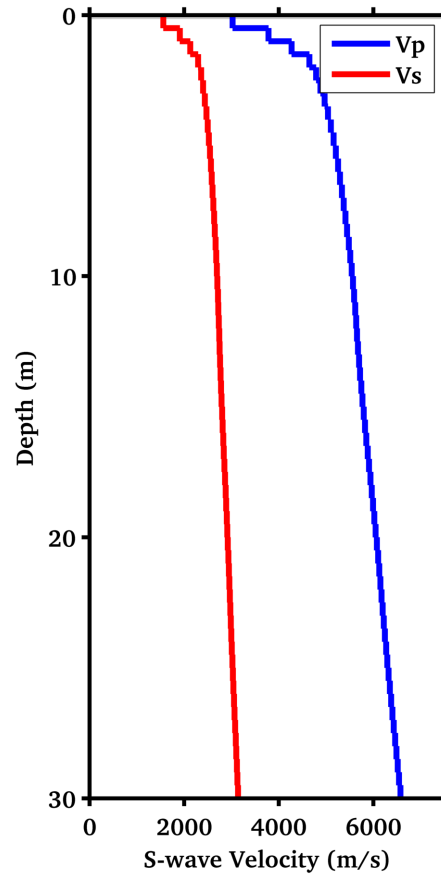


Figure 4 - Final summary models (V_s and V_p) for the free surface and the tunnel. V_p profile is obtained converting V_s values using the log-linear relation in **Figure 3**. It has to be noticed that in B the decrease in velocity in proximity of the gallery is realistically explainable by the stress release and fracturing induced by excavation.

6. Amplification models

Site amplification functions have been computed using two different approaches: the S-wave transfer function for vertical propagation and the quarter-wavelength amplification. In general the first method is used to evaluate the resonance characteristics of the site, while the second is more useful to assess the effect of the velocity contrasts between the lowermost rock layer (as reference) and the different QWL averaging depths. The two amplification functions are then corrected for the Swiss rock reference velocity profile as defined in Poggi et al. (2011), according to the procedure described in Edwards et al. (2013). Given the lower velocities in the uppermost part of the EMMET profile compared to the Swiss reference, the final corrected amplification function shows a lower average amplification level at high frequencies than the uncorrected (**Figure 7**).

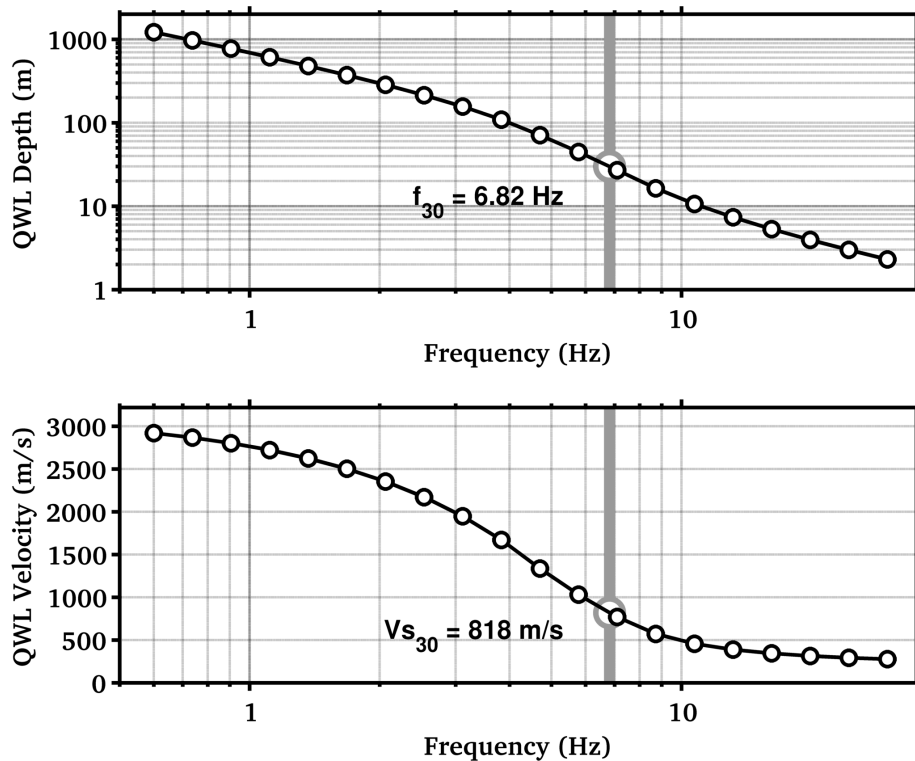


Figure 5 - Quarter-wavelength representation of the summary S-wave velocity profile at the free-surface. Top: the depth-frequency dependency. Bottom: the QWL average velocity. The V_{s30} value is indicated with its corresponding QWL frequency.

Amplification functions using the transfer function and the quarter-wavelength approach are comparable (**Figure 8**), even if the transfer function provides a slightly larger amplification, because of the presence of some weak resonance peaks. At low frequencies both methods converge to the same amplification level. It has to be notice that the amplification functions do not include attenuation at this stage of the analysis, as the quality factors of the site are unknown.

Amplification function has also been computed at the depth of the tunnel from the extended velocity profile (free surface plus tunnel model, **Figure 9**) using the SH transfer function formalism. With respect to the amplification computed assuming free-surface conditions (Figure 7), the ground motion model obtained when accounting for the full-wave propagation along the extended profile presents the typical troughs due to negative interference of up-going and down-going reflected waves.

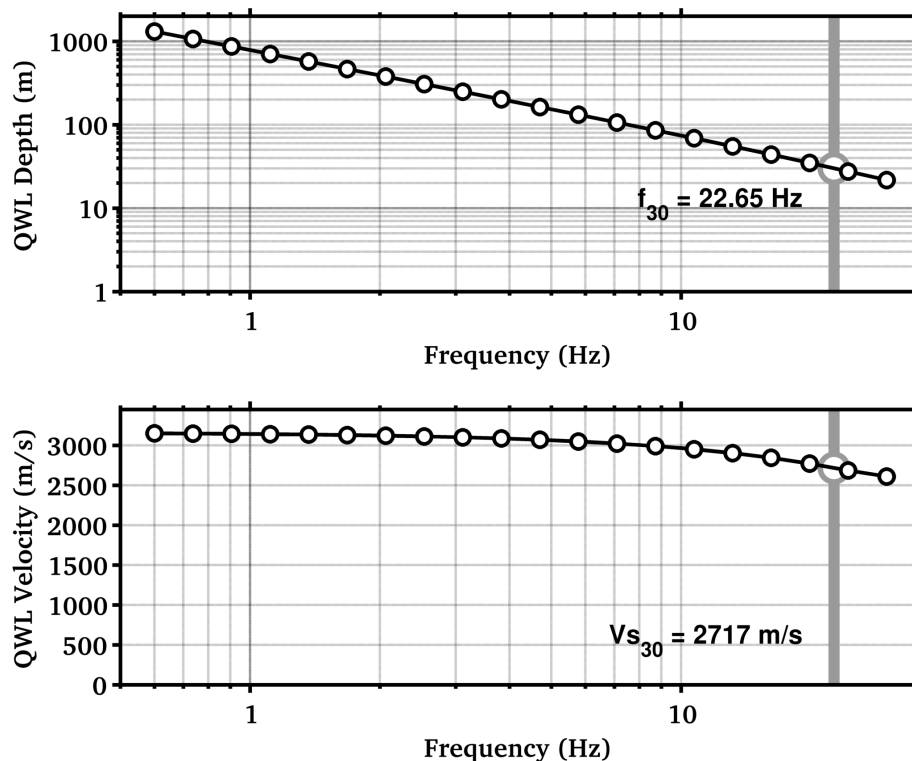


Figure 6 - Quarter-wavelength representation of the summary S-wave velocity profile within the tunnel. Top: the depth-frequency dependency. Bottom: the QWL average velocity. The V_{s30} value is indicated with its corresponding QWL frequency.

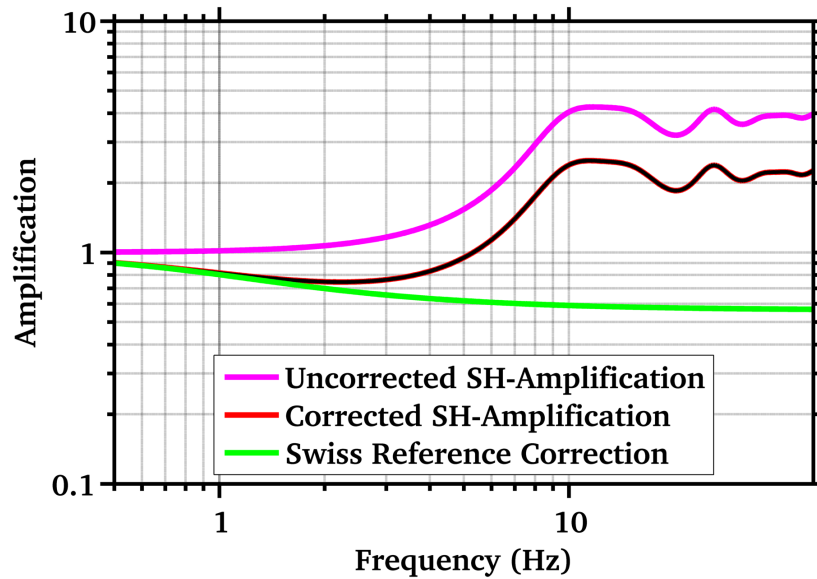
Averaging depth (m)	Vs-mean (m/s)	St.Dev.
5	336.6193	--
10	442.717	--
15	544.2156	--
20	640.811	--
25	732.5255	--
30	817.9385	--
40	969.0425	--
50	1098.196	--
75	1376.764	--
100	1602.18	--
150	1916.331	--
200	2124.626	--

Table 1 - Average travel-time velocities at different depths of the free-surface velocity model. Vs30 is highlighted.

Averaging depth (m)	Vs-mean (m/s)	St.Dev.
5	2211.929	--
10	2399.862	--
15	2505.403	--
20	2585.154	--
25	2654.243	--
30	2717.461	--
40	2816.634	--
50	2879.79	--
75	2968.541	--
100	3014.999	--
150	3062.935	--
200	3087.479	--

Table 2 - Average travel-time velocities at different depths of the tunnel velocity model. Vs30 is highlighted.

A) Free-surface profile



A) Tunnel profile

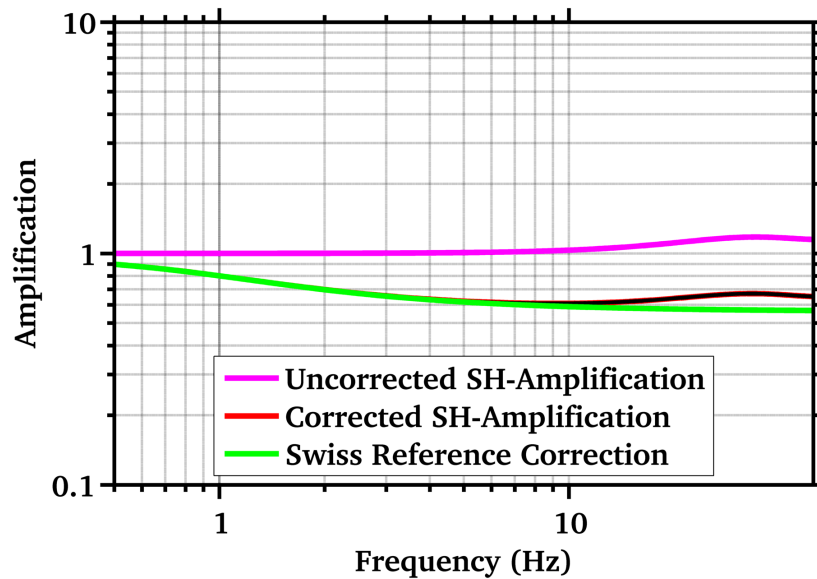
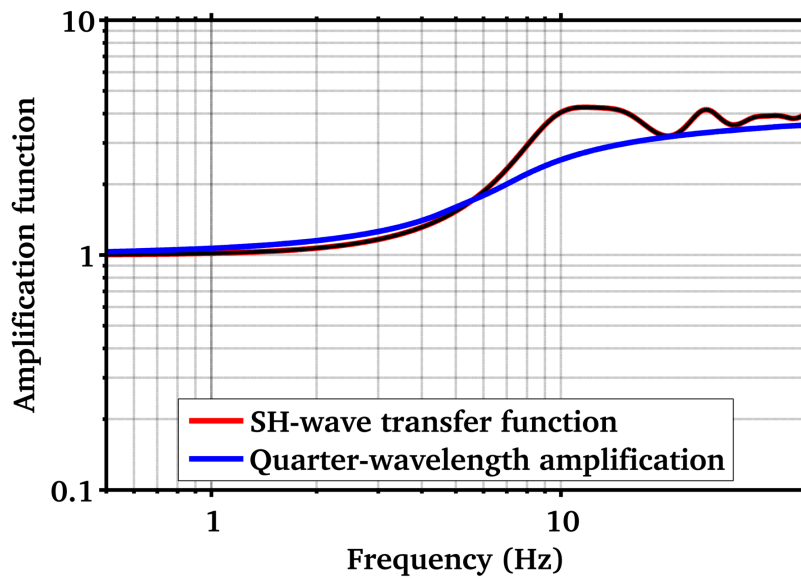


Figure 7 - Correcting the SH-wave transfer function for the Swiss (rock) reference conditions (Poggi et al. 2011). The final corrected amplification function shows a lower (average) amplification at high frequencies than the uncorrected.

A) Free-surface profile



A) Tunnel profile

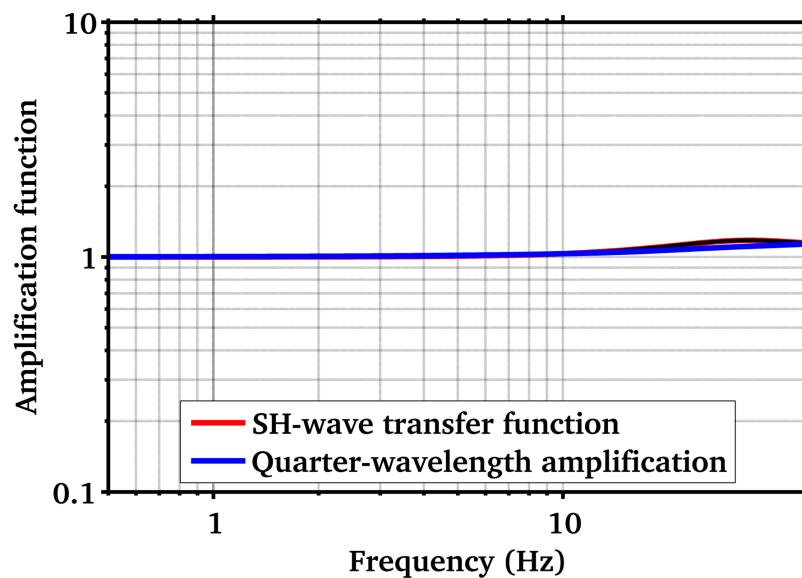


Figure 8 - Comparison of amplification functions computed using the SH-wave transfer function and the quarter-wavelength formalism on the inverted velocity models (in this case functions are not corrected for the Swiss reference conditions).

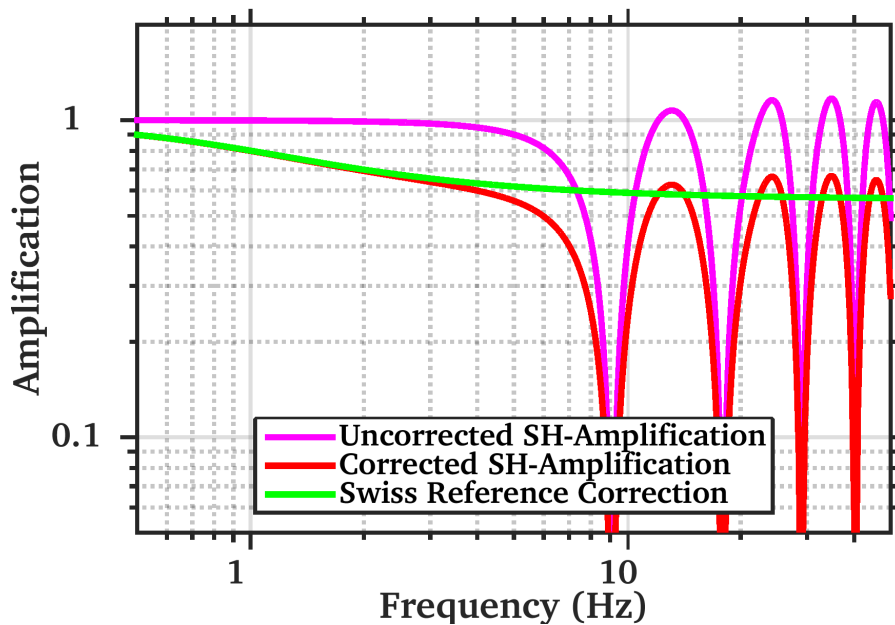


Figure 9 - Amplification functions computed at the depth of the tunnel using the extended profile (free surface plus tunnel). Negative peaks induced by destructive interferences of reflected phases from the surfaces are clearly visible.

REFERENCES

- Edwards, B., C. Michel, V. Poggi and D. Fäh (2013). Determination of Site Amplification from Regional Seismicity: Application to the Swiss National Seismic Networks. Accepted for publication in *Seismological Research Letters*.
- Joyner, W. B., R. E. Warrick and T. E. Fumal (1981). The Effect of Quaternary Alluvium on Strong Ground Motion in the Coyote Lake, California, Earthquake of 1979, *Bulletin of the Seismological Society of America*, 71, 1333-1349.
- Poggi, V., B. Edwards and D. Fäh (2011). Derivation of a Reference Shear-Wave Velocity Model from Empirical Site Amplification, *Bulletin of the Seismological Society of America*, 101, 258-274.

APPENDIX A

Active Seismic report